

Magnetic anisotropy and spin wave relaxation in CoFe/PtMn/CoFe trilayer films

Y. H. Ren,^{1,a)} C. Wu,¹ Y. Gong,¹ C. Pettiford,² and N. X. Sun²

¹*Department of Physics and Astronomy, Hunter College, the City University of New York, 695 Park Avenue, New York, New York 10065, USA*

²*Electrical and Computer Engineering, Northeastern University, 409 Dana Research Center, 360 Huntington Avenue, Boston, Massachusetts 02115, USA*

(Received 13 January 2009; accepted 3 February 2009; published online 6 April 2009)

We investigated the magnetic anisotropic properties and the spin wave relaxation in trilayer films of CoFe/PtMn/CoFe grown on the seed layer Ru or NiFeCr with CoFe compositions being Co-16 at. % Fe. The measurements were taken in samples with the ferromagnetic layers of CoFe varying from 10 to 500 Å by the ferromagnetic resonance (FMR) technique. The magnetic anisotropic parameters were investigated by rotating the field aligned axis with respect to the spectral field in the configurations of both in plane and out of plane. We determine the effective in-plane anisotropy field of ~ 0.005 T, the uniaxial out-of-plane anisotropy of ~ -0.3 T, and the exchange stiffness D of ~ 512 meV Å². Moreover, spin wave damping was estimated by analyzing the FMR linewidth and line shape as a function of the angle between the external field and easy axis and as a function of the thickness of the CoFe layers. We identify an extrinsic contribution of the damping parameter dominated by two-magnon scattering in addition to the intrinsic Gilbert term with a damping parameter, $\alpha=0.012$. Further, we reveal that a significant linewidth broadening could also be caused by the overlap of the surface and the uniform spin wave excitations. The FMR lines show a strong dependence of the surface anisotropy contribution of free energy in trilayer films. © 2009 American Institute of Physics. [DOI: [10.1063/1.3093927](https://doi.org/10.1063/1.3093927)]

I. INTRODUCTION

Soft magnetic multilayer films have attracted a lot of attention most recently because of their potential applications in magnetic sensors and rf/microwave devices.¹⁻⁴ As a result of the interfacial interaction and/or the exchange coupling, the sandwiched films show excellent magnetic softness with a uniaxial anisotropy field and a low coercivity.⁵ One such example is the Ru-seeded CoFe/PtMn/CoFe structure.^{6,7} The high moment ferromagnetic (FM) CoFe thin films couple strongly with the antiferromagnetic (AFM) PtMn layer, rendering a low hard axis coercivity of 2–4 Oe and a significant enhancement of in-plane anisotropy of 57–123 Oe.^{6,7} More interestingly, the trilayer can achieve a low ferromagnetic resonance (FMR) linewidth together with the significantly enhanced anisotropy field, in contrast to exchange-coupled FM/AFM bilayers. These properties make the material a promising candidate for rf/microwave operations.

The dynamical response of magnetization at rf/microwave frequencies provides reliable micromagnetic descriptions of multilayer-based devices. So far, there is significant progress on the understanding of dynamical properties of exchange-coupled FM/AFM bilayers and the physical contributions to the FMR resonant field and linewidth.⁸⁻¹¹ However, little is known about the dynamic magnetic properties of FM/AFM/FM structures, e.g., Gilbert damping, two-magnon scattering processes, and exchange coupling interactions between FM layers, which are of great importance to assess the technological potential of these materials. Mag-

netization dynamics in film structures can be carried out by various experimental techniques, such as ultrafast magneto-optical Kerr effect, Brillouin light scattering, and FM resonance. The resonant field and linewidth measured in FMR provide direct information on the spin wave resonance and damping in magnetic materials and consequently lead to insights on the microscopic interactions.

In this paper, we report on the magnetic properties including effective magnetic anisotropy fields, Gilbert damping, two-magnon scattering, and exchange stiffness in two series of multilayer CoFe/PtMn/CoFe films grown on the seed layer Ru or NiFeCr with CoFe compositions being Co-16 at. % Fe. The FMR measurements were taken in samples with the FM CoFe layer thicknesses that were varied from 10 to 500 Å. The magnetic anisotropic parameters were determined by rotating the field aligned axis with respect to the spectral field in the configurations of both in plane and out of plane. We obtain the effective in-plane anisotropy field of ~ 0.005 T, the uniaxial out-of-plane anisotropy of ~ -0.3 T, and the exchange stiffness D of ~ 512 meV Å² at room temperature. In addition, we analyzed the resonance linewidth of CoFe/PtMn/CoFe by the thickness dependence of the CoFe layers. We realize that the spin wave relaxation could be described in terms of two independent contributions: they are the intrinsic mechanism dominated by Gilbert damping and the extrinsic mechanism dominated by two-magnon scattering. Moreover, we reveal that a significant linewidth broadening could also be caused by the overlap of the surface and the uniform spin wave excitations. The surface anisotropy contribution is found to be critical in understanding the FMR lines.

^{a)}Electronic mail: yre@hunter.cuny.edu.

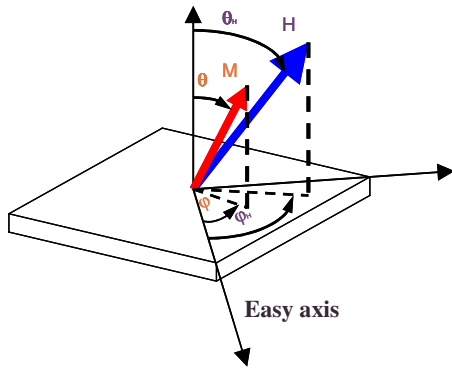


FIG. 1. (Color online) The polar coordinate system used in our discussion.

II. EXPERIMENTS

FM/AFM/FM trilayers of CoFe/PtMn/CoFe seeded with 30 Å of Ru or NiFeCr were deposited on oxidized silicon coupons by dc magnetron sputtering with base pressures in the order of 10^{-9} Torr.⁶ The sample configuration is illustrated in the inset of Fig. 2. The thicknesses of FM CoFe layers were varied from 10 to 500 Å, while that of the AFM PtMn layer was fixed at 120 Å. Magnetic field annealing was carried out for these films to induce a uniaxial anisotropy field by exchange coupling before characterizing these films. Magnetic fields such as coercive fields and exchange coupling fields were all measured with a vibrating sample magnetometer (VSM) with an error of 1 Oe. The FMR measurements were carried out at the X-band of 9.74 GHz using a Bruker EMX electron paramagnetic resonance spectrometer. The polar coordinate system used in the subsequent discussion is plotted in Fig. 1. The orientation of the dc magnetic field H is described by θ_H and ϕ_H , and the resulting equilibrium orientation of the magnetization M is given by θ and ϕ . The samples were placed in a quartz tube inserted in the microwave cavity and rotated with respect to H in an orientation either in the layer plane (change ϕ) or along the out-of-plane configuration (between the in-plane orientation $\theta_H = 90^\circ$ and the normal to the layer plane $\theta_H = 0^\circ$).

III. RESULTS AND DISCUSSION

A. Ferromagnetic resonance fields and magnetic anisotropic parameters

Figure 2(a) shows FM resonance spectra for various magnetic field orientations in a sample with 200 Å layers of CoFe in the out-of-plane configuration. As the direction of the magnetic field approaches the film normal, the resonance line shifts a few kOe to a higher field, and we observe a significant broadening of FMR linewidth (as a result, its amplitude decreases). The line shift is induced by the demagnetizing field. For a thin film sample, a macroscopic magnetization could produce a field of $4\pi M$, which usually points along the perpendicular direction of the sample plane. When we rotate our sample with respect to the applied magnetic field, the equilibrium angle of the magnetization vector depends strongly on the external field value. Therefore, we expect to see a shift of FMR field and an increase in linewidth at an intermediate angle. This effect is more obvious in the

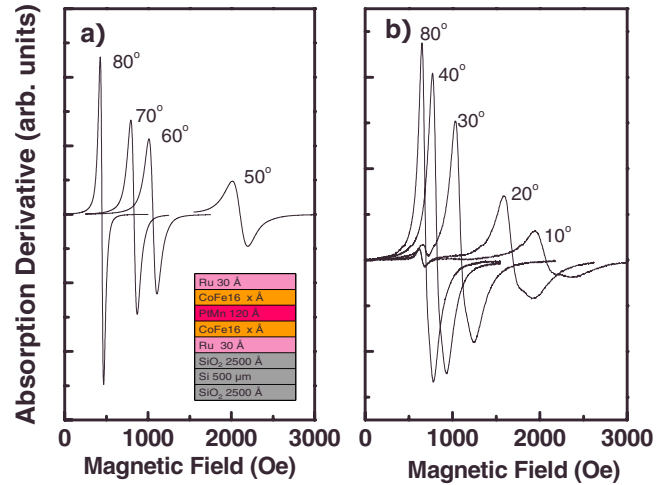


FIG. 2. (Color online) Spin wave resonance spectra for various magnetic field orientations in the sample (a) with 200 Å layers of CoFe and (b) with 400 Å layers of CoFe in the out-of-plane configuration. The inset shows the sample configuration.

FMR spectra of the sample with 400 Å layers of CoFe, which could be explained by the excitation of an exchange-dominated surface spin wave excitation. As shown in Fig. 2(b), in addition to the observation of the FMR line shift and broadening, we notice a significant change in the line shape. The lines show strong asymmetric behaviors with respect to the base line. The asymmetric behavior of the absorption curve could come from the overlap of the surface and uniform spin wave excitations. As discussed by Vittoria¹² and McKnight and Vittoria,¹³ the surface impedance shows a strong dependence on the thickness of the FM layers as well as the interlayer exchange coupling between layers, therefore, on the angle between the external field and film normal.

We use the FMR resonance lines and their linewidths to determine the magnetic properties of the trilayers of CoFe/PtMn/CoFe. We employ the Landau-Lifshitz-Gilbert equation of motion to describe our results,¹⁴⁻¹⁶

$$\frac{dM}{dt} = \gamma M \times [H - \nabla_M F_A + DM^{-1} \nabla^2 M] - \frac{\alpha}{\gamma M_s} M \times \frac{dM}{dt}, \quad (1)$$

where $F_A = \sum_{i=1,2} (-2\pi M_i^2 t_F \sin^2 \theta_i - K_{UF} \cos^2 \theta_i - K_A t_F \sin^2 \theta_i \sin^2 \phi_i - M_i H_{ei} \cos \theta_i \cos \phi_i) + JM_1 \cdot M_2$ is the demagnetization field, the magnetic anisotropy, and the interlayer exchange contributions for the FM layers to the free energy.¹⁷⁻¹⁹ t_F is the thickness of the FM layers, K_U and K_A are the out-of-plane uniaxial and the effective in-plane anisotropy constants, H_e is the exchange bias field between the CoFe and PtMn layers, J describes the interlayer exchange coupling between the CoFe layers, H is the external field, M_s is the saturation magnetization, and γ is the gyromagnetic factor. α is the dimensionless damping coefficient (Gilbert damping constant), and D is the spin stiffness describing the exchange interactions in the films. The excitation of the spin waves is due to the absorption of microwaves.

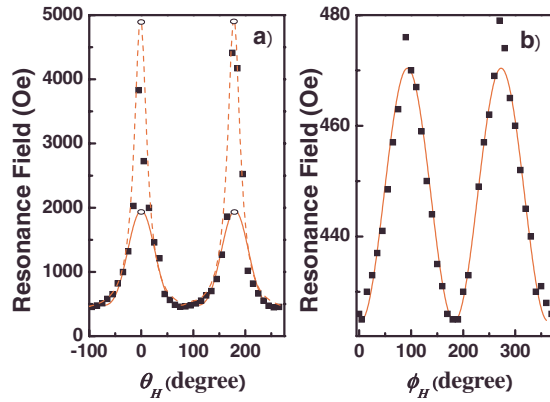


FIG. 3. (Color online) Angular dependences of resonance fields of the FMR mode in both (a) the out-of-plane and (b) the in-plane configurations for the sample with 400 Å layers of CoFe. The solid lines show the fits using Eqs. (2) and (3). The dashed line in (a) shows a new fit after compensating the surface and interface anisotropy into the free energy density. The resonant field at $\theta_H=0^\circ$ is a singularity and cannot be reached.

Indeed, when the applied field rotates along the out-of-plane direction (keep $\phi=0^\circ$), the resonance frequency follows

$$f_{\text{FMR}}^2 = \left(\frac{\gamma}{2\pi}\right)^2 \left[H_R \cos(\theta_H - \theta) - \left(4\pi M_S - \frac{2K_U}{M_S}\right) \cos 2\theta \pm Dk^2 \right] \times \left[H_R \cos(\theta_H - \theta) + \left(-4\pi M_S + \frac{2K_U}{M_S}\right) \cos^2 \theta - \frac{2K_A}{M_S} \pm Dk^2 \right], \quad (2)$$

where H_R is the resonance field, $4\pi M_S - 2K_U/M_S$, the saturation magnetization reduced by the uniaxial perpendicular anisotropy field gives an effective magnetization, and k is the effective wave vector of a spin wave mode. For all studied thicknesses, we neglect the exchange bias field between the CoFe layer and the PtMn layer according to the VSM hysteresis results on the CoFe/PtMn/CoFe samples.⁶ The inter-layer exchange interaction between the CoFe layers is small due to their large separation.

As the applied field and the magnetization are along the in-plane direction, the resonance frequency follows:

$$f_{\text{FMR}}^2 = \left(\frac{\gamma}{2\pi}\right)^2 \left(H_R - \frac{2K_A}{M_S} \cos 2\phi \pm Dk^2 \right) \times \left(H_R + 4\pi M_S - \frac{2K_U}{M_S} + \frac{2K_A}{M_S} \sin^2 \phi \pm Dk^2 \right). \quad (3)$$

Figures 3(a) and 3(b) show the plots of the angular dependences of the resonance field of the FMR mode and their fitting (the solid lines) using Eqs. (2) and (3) in the sample with 400 Å layers of CoFe in the out-of-plane and in-plane configurations, respectively. As seen by the nonsinusoidal shape of the angular dependence in Fig. 3(a) (out-of-plane configuration), we realize that the magnetic fields at which FMR is observed are not high enough to turn the magnetiza-

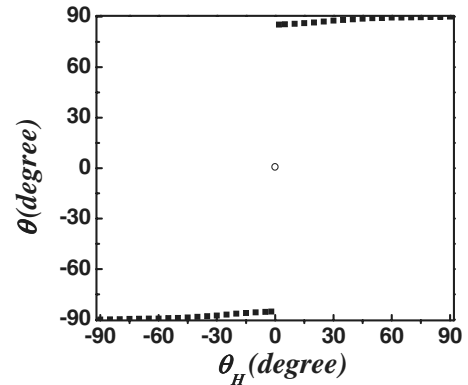


FIG. 4. Equilibrium angle of the magnetization as a function of angle of the applied field in the out-of-plane configuration ($\phi_H=0^\circ$).

tion vector M parallel to the magnetic field H when the latter has an out-of-plane component. We examine the equilibrium angles of the magnetization by minimizing the free energy density. The result shown in Fig. 4 indicates that the direction of M immediately begins to seek the easy orientation as the magnetic field is tilted away from the direction normal to the sample surface (the resonant field at $\theta_H=0^\circ$ is a “singularity” and cannot be reached). In contrast to that of the out-of-plane configuration, the resonant magnetic fields are sufficiently high to turn the magnetization vector M parallel to the magnetic field H in the in-plane orientations. As shown in Fig. 3(b), a clear twofold symmetry for the in-plane geometry corresponds to the uniaxial anisotropy field induced by the magnetic field annealing. We obtained the following parameters: $\gamma=1.835 \times 10^{11}$ Hz/T, $4\pi M_S - 2K_U/M_S=2.4$ T, and $2K_A/M_S \sim 50$ Oe. The values are consistent with those from our VSM measurements that give us a saturated magnetization of ~ 2.1 T and an in-plane anisotropy of ~ 57 Oe.⁶ In the meantime, we notice that the experimental resonance data show a strong deviation from the theoretical prediction in the out-of-plane configuration [Fig. 3(a)], particularly when external magnetic field, H , is oriented close to the perpendicular direction of the film. The difference is attributed to the contribution of surface anisotropy. We will discuss this in the later session.

B. Ferromagnetic resonance linewidth and magnetization relaxation

Further, we investigate the magnetization relaxation (damping) from the FMR linewidths in these trilayer structures. The measured resonance linewidth, ΔH_{pp} , is the sum of the intrinsic Gilbert damping contribution, ΔH_{in} , and extrinsic inhomogeneous line broadening, ΔH_{ex} . The intrinsic FMR linewidth is derived from the free energy density, F by the relation:²⁰

$$\Delta H_{in} = \frac{2}{\sqrt{3}} \times \frac{1}{\left| \frac{\partial \omega}{\partial H_{res}} \right|} \times \frac{\alpha \gamma}{M_S} \left(\frac{\partial^2 F}{\partial \theta^2} + \frac{1}{\sin^2 \theta} \times \frac{\partial^2 F}{\partial \phi^2} \right). \quad (4)$$

Figure 5 illustrates the FMR linewidth as a function of the in-plane angle ϕ between the applied field and the easy

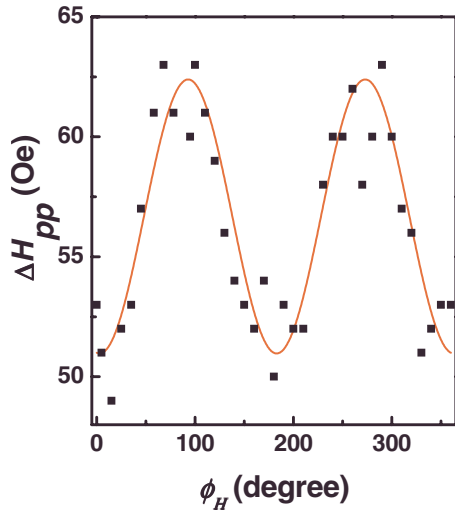


FIG. 5. (Color online) FMR linewidth as a function of in-plane angle ϕ between the applied field and the easy axis for the sample with 400 Å layers of CoFe.

axis in the sample with 400 Å layers of CoFe. The solid line shows a fit by using Eq. (4). The good consistency between the experimental data and the fit shows that our measured resonance linewidth, ΔH_{pp} is mostly governed by the phenomenological Gilbert damping. We calculate the Gilbert damping parameter α according to the above equation. We obtain an α of ~ 0.012 . The parameter α is independent of the thickness of CoFe layers and the value of resonance frequency. This behavior agrees with the nature of the Gilbert damping.

In addition to the intrinsic mechanism in the damping parameter, we also see an extrinsic contribution on the magnetization relaxation when we further measured the FMR linewidths of samples with thinner layers of CoFe. The extrinsic contribution generally includes two-magnon scattering and so-called inhomogeneous linewidth broadening caused by nonuniformities of the magnetic properties in the measured volume.²¹ Here, we neglect the influence of linewidth broadening due to locally nonuniform material properties since the resonant field, H_{res} , is much larger than 500 Oe. This outweighs the varying anisotropic field on a millitesla scale in the trilayer samples. While the intrinsic linewidth, ΔH_{in} , does not depend on the resonance frequency at the corresponding H_{res} field, the two-magnon scattering due to fluctuations of the interlayer exchange coupling shows a strong thickness dependence on the FM layers.¹⁰ Most recently, Rezende *et al.*¹⁹ deduced that the rates of spin wave relaxation measured by FMR can be fitted with a t^{-2} dependence plus a constant term if one includes both the intrinsic mechanism dominated by the Gilbert damping and the extrinsic mechanism dominated by the two-magnon scattering.

We use the t^{-2} dependence to estimate the contribution from the two-magnon scattering by studying the linewidths of CoFe trilayer samples with various thicknesses of the FM CoFe layers. Figure 6 shows the FMR linewidth, ΔH_{pp} , as a function of the thickness t of FM layers in two CoFe trilayer sample series grown with seed layers of Ru and NiFeCr, separately. The magnetic field is applied along their easy-axis direction. We fit the data by the t^{-2} dependence shown

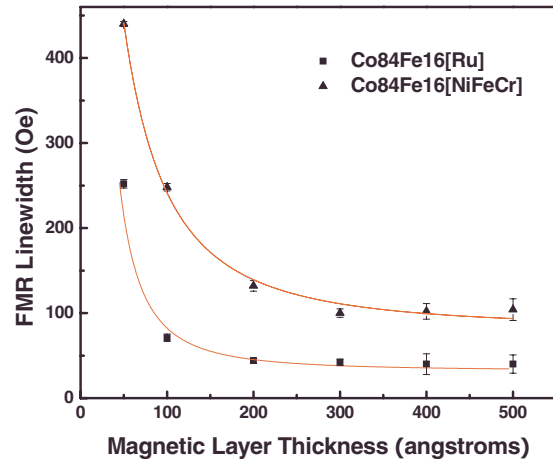


FIG. 6. (Color online) FMR linewidth (ΔH_{pp}) as a function of the thickness t of FM layers in two CoFe trilayer sample series grown with seed layers of Ru and NiFeCr. The solid lines are the t^{-2} fits.

as solid lines. The agreement between the fit and experimental results indicates an extrinsic origin, dominated by two-magnon scattering processes. Moreover, it is important to notice a significant linewidth broadening in the NiFeCr-seeded CoFe layers as compared to those of the Ru-seeded samples. As the Ru seed layers were replaced by NiFeCr, only the interface properties were modified. Our result shows that the surface and interface properties of multilayer structures are crucial in understanding the spin wave resonance and the processes of spin wave relaxation.

IV. SURFACE MAGNETIC ANISOTROPY AND DYNAMICAL SURFACE PINNING

It is well established that the interfacial and surface contributions are very important in analyzing the FMR field and linewidth of the magnetic trilayer structures.^{12,13,21,22} As illustrated in Fig. 7, the broad feature at the high field side of the main mode can be deconvoluted by a weak absorption line that is attributed to an exchange-dominated nonpropa-

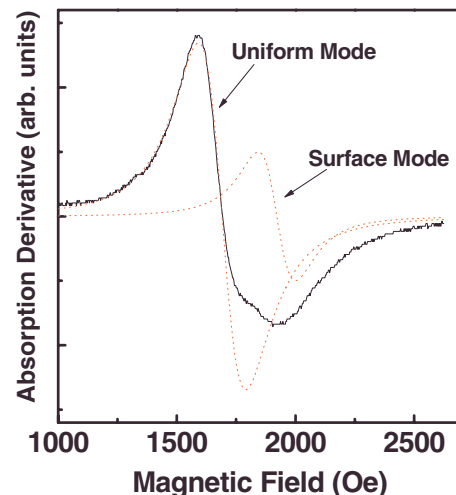


FIG. 7. (Color online) A typical FMR spectrum observed in the sample with 400 Å layers of CoFe close to the out-of-plane magnetic field orientation. The dashed lines show the deconvolution of the spectrum, indicating a uniform mode and a surface spin wave mode.

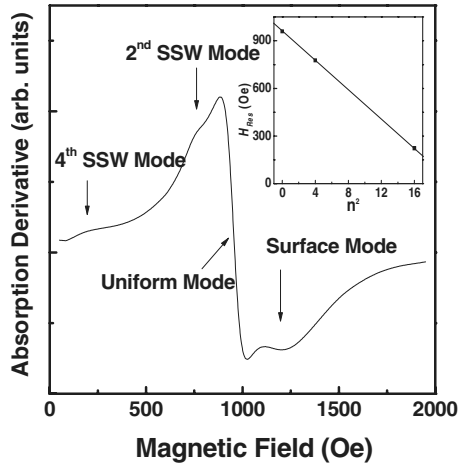


FIG. 8. A FMR spectrum in the eight period CoFe trilayer structure. The arrows show different spin wave modes. The inset shows a dependence of H_n measured at the out-of-plane configuration on the square of the corresponding mode number, n^2 . The line is a linear fit.

gating surface mode. The surface mode disturbs the main resonance line and introduces an additional contribution of the FMR linewidth and an asymmetric line shape. Several groups have discussed the double peak feature in FM samples in terms of the existence of surface uniaxial anisotropy.^{22–26} For example, Teale and Pelegrini²³ deduced that for parallel geometry the surface mode shifted from the bulk mode to higher fields with increasing positive values of the surface anisotropy constant. This corresponds to an easy-axis normal to the sample surface. Wang *et al.*²⁴ revealed that a negative contribution to the spin wave energy could be introduced by the surface anisotropy.

Here, we study the surface and interface properties of the trilayer samples by means of the surface spin wave and standing spin wave (SSW) excitations. For a configuration close to out of plane ($\theta \sim 10^\circ$), in addition to a broad band feature on the high field side of the spectrum, which is attributed to an exchange-dominated nonpropagating surface mode, three FMR lines can be well resolved in the eight period structure of CoFe trilayers, as shown in Fig. 8. These lines are identified as the uniform spin wave mode and high-order SSW modes. We analyze the spin wave structure according to the change in the boundary conditions. In particular, as shown in the inset in Fig. 8, the positions of FMR lines for the sample are characterized by a mode separation that varies quadratically with n . The result implies that spin precession of the spin waves at the surface is nearly free. This represents the so-called free boundary conditions, in which the position of the n th FMR line is given by

$$H_n = H_0 - n^2 \frac{D\pi^2}{g\mu_B L^2}, \quad (5)$$

where H_0 is the position of the theoretical uniform mode, μ_B is the Bohr magneton, n is an even integer ($n=0, 2, 4$), and L is the total thickness of the CoFe layers. The observation of the high-order even SSW modes in the eight period sample is due to the effective coupling between the CoFe layers. The antisymmetric modes (odd modes: $n=1, 3, 5$) cannot be measured in our FMR technique since in uniform

thin films FMR selection rules allow only excitations with a net magnetic moment. The exchange stiffness D (which gives a measure of the strength of exchange interaction that tries to keep magnetic moments parallel) can then be determined from a linear fit shown in the inset in Fig. 8: $D \sim 512 \text{ meV } \text{\AA}^2$, which can also be represented as $D/g\mu_B \sim 42.03 \text{ T nm}^2$.

Moreover, we realize that the separation between the uniform spin wave mode and SSW mode depends strongly on the relative rotation angle, θ , with respect to the perpendicular direction of the film plate. As shown in Fig. 2(b), as we rotate H away from $\theta=0^\circ$, the high-order standing mode gradually loses its intensity. Eventually, at a critical angle, θ_C ($\sim 40^\circ$), the multiple spin wave spectrum vanishes except for the single narrow resonance line due to the uniform spin wave excitation. We note that the complex behavior of the angular dependence of the FMR spectrum described above shows some similarities to those previously reported in Permalloy,^{27,28} in half-metallic FM films,²⁹ and recently in diluted magnetic semiconductors.^{24,26} The results could be related to the change in surface spin pinning as discussed below.

According to Puzskarski's²² surface inhomogeneity SI model, the actual eigenmodes are selected by the boundary conditions, which in turn depend on the dynamical surface spin pinning condition. We could include an effective surface anisotropy field (K_{surf}) to explain our results. Following the theory of surface states in FMR, the change in spin energy at each film surface and interface can be described by an effective parameter,

$$K_S(\theta, \phi) = \frac{dM}{z} (\vec{m} \cdot \vec{K}_{\text{surf}}), \quad (6)$$

where z is the number of nearest-neighbor spins in a crystal lattice, d is the lattice constant, and \vec{m} is the unit vector of magnetization. The value of K_S gives us a measurement of the strength of the spin pinning at the surface and can be used to qualitatively explain our angular dependent FMR spectra: As we rotate H away from the perpendicular direction of the layer plane, K_S changes accordingly due to the change in the magnetization direction (\vec{K}_{surf} is a constant vector). This leads to the change in the surface boundary condition, which gives us a different value of the wave vector k . In turn, we will have a relative shift of FMR lines and relative intensity change between spin wave modes.

In addition, the uniform spin wave mode can also be shifted if we consider the contribution of the surface anisotropy field in the free energy density. As discussed by Puzskarski,²² the energy of all the spins present per unit area of the surface can be written as

$$E_S = - \frac{Sg\mu_B}{d^2} (\vec{m} \cdot \vec{K}_{\text{surf}}), \quad (7)$$

where S is the atom spin. Since \vec{m} rotates with external magnetic field, we have E_S changing with the orientation of H . The dashed line in Fig. 3(a) shows a new fit after compensating the surface and interface anisotropy into the free energy density. The good fit of the experimental data obtained

by including the surface energy reveals that we need to consider the energy contribution from the surface spin excitations. This is extremely important in designing magnetoelectronic devices based on nanoscale structures.

V. CONCLUSION

In summary, we investigated the magnetic properties including effective magnetic anisotropies, Gilbert damping, two-magnon scattering, and exchange interactions in a series of multilayer CoFe/PtMn/CoFe films grown on the seed layer Ru and NiFeCr with CoFe compositions being Co-16 at. % Fe. The FMR measurements were taken for samples with the FM CoFe layer thicknesses varying from 10 to 500 Å. The magnetic anisotropic parameters were determined by rotating the field aligned axis with respect to the spectral field in the configurations of both in plane and out of plane. We obtain the effective in-plane anisotropic field of ~ 0.005 T, the uniaxial out-of-plane anisotropy field of ~ -0.3 T, and the exchange stiffness D of ~ 512 meV Å². Moreover, the measured resonance linewidth of CoFe/PtMn/CoFe was analyzed by the thickness dependence of the CoFe layers. We realize that the spin wave relaxation could be described in terms of two independent contributions: they are the intrinsic mechanism dominated by Gilbert damping and the extrinsic mechanism dominated by two-magnon scattering. Finally, we reveal that the significant linewidth broadening could be caused by the overlap of the surface and the uniform spin wave modes, and the surface anisotropy energy is critical in understanding the FMR lines.

ACKNOWLEDGMENTS

We are grateful to Dr. X. Liu (Notre Dame) for illuminating discussions. We also thank Professor Steve Greenbaum for allowing us to use his EPR/FMR facilities. This work is supported in part by the Petroleum Research Fund and PSC-CUNY Award.

- ¹B. Kuanr, Z. Celinski, and R. E. Camley, *Appl. Phys. Lett.* **83**, 3969 (2003); B. Kuanr, D. L. Marvin, T. M. Christensen, R. E. Camley, and Z. Celinski, *ibid.* **87**, 222506 (2005).
- ²M. Yamaguchi, S. Arakawa, H. Ohzeki, Y. Hayashi, and K. I. Arai, *IEEE Trans. Magn.* **28**, 3015 (1992).
- ³A. M. Crawford, D. Gardner, and S. X. Wang, *IEEE Trans. Magn.* **38**, 3168 (2002).
- ⁴B. Viala, A. S. Royet, R. Cuchet, M. Aid, P. Gaud, O. Valls, M. Ledieu, and O. Acher, *IEEE Trans. Magn.* **40**, 1999 (2004).
- ⁵S. X. Wang, N. X. Sun, M. Yamaguchi, and S. Yabukami, *Nature (London)* **407**, 150 (2000).
- ⁶C. Pettiford, A. Zeltser, S. Z. D. Yoon, V. G. Harri, C. Vittoria, and N. X. Sun, *J. Appl. Phys.* **99**, 08C901 (2006).
- ⁷C. Wu, A. N. Khalfan, C. Pettiford, N. X. Sun, S. Greenbaum, and Y. H. Ren, *J. Appl. Phys.* **103**, 07B525 (2008).
- ⁸R. D. McMichael, M. D. Stiles, P. J. Chen, and W. F. Egelhoff, Jr., *Phys. Rev. B* **58**, 8605 (1998).
- ⁹D. J. Twisselmann and R. D. McMichael, *J. Appl. Phys.* **93**, 6903 (2003).
- ¹⁰S. M. Rezende, M. A. Lucena, A. Azevedo, F. M. de Aguiar, J. R. Fermin, and S. S. P. Parkin, *J. Appl. Phys.* **93**, 7717 (2003).
- ¹¹S. M. Rezende, A. Azevedo, M. A. Lucena, and F. M. de Aguiar, *Phys. Rev. B* **63**, 214418 (2001).
- ¹²C. Vittoria, *Phys. Rev. B* **32**, 1679 (1985).
- ¹³S. W. McKnight and C. Vittoria, *Phys. Rev. B* **36**, 8574 (1987).
- ¹⁴P. E. Wigen, *Phys. Rev.* **133**, A1557 (1964).
- ¹⁵B. Heinrich, *Ultrathin Magnetic Structures* (Springer, Berlin, 1994), Vol. I; B. Heinrich, *Ultrathin Magnetic Structures* (Springer, Berlin, 2005), Vol. II.
- ¹⁶M. Farle, *Rep. Prog. Phys.* **61**, 755 (1998).
- ¹⁷R. J. Hicken, A. Barman, V. V. Kruglyak, and S. Ladak, *J. Phys. D* **36**, 2183 (2003).
- ¹⁸H. W. Xi and R. M. White, *Phys. Rev. B* **62**, 3933 (2000).
- ¹⁹S. M. Rezende, A. Azevedo, F. M. de Aguiar, J. R. Fermin, W. F. Egelhoff, and S. S. P. Parkin, *Phys. Rev. B* **66**, 064109 (2002).
- ²⁰H. Suhl, *Phys. Rev.* **97**, 555 (1955).
- ²¹R. Arias and D. L. Mills, *Phys. Rev. B* **60**, 7395 (1999).
- ²²H. Puzskarski, *Prog. Surf. Sci.* **9**, 191 (1979).
- ²³R. W. Teale and F. Pelegriani, *J. Phys. F: Met. Phys.* **16**, 621 (1986).
- ²⁴D. M. Wang, Y. H. Ren, X. Liu, J. K. Furdyna, M. Grimsditch, and R. Merlin, *Phys. Rev. B* **75**, 233308 (2007).
- ²⁵G. T. Rado and R. J. Hicken, *J. Appl. Phys.* **63**, 3885 (1988).
- ²⁶X. Liu, Y. Sasaki, and J. K. Furdyna, *Phys. Rev. B* **67**, 205204 (2003); X. Liu, Y. Y. Zhou, and J. K. Furdyna, *ibid.* **75**, 195220 (2007).
- ²⁷T. D. Rossing, *J. Appl. Phys.* **34**, 1133 (1963).
- ²⁸J. Gomez, A. Butera, and J. A. Barnard, *Phys. Rev. B* **70**, 054428 (2004).
- ²⁹B. Rameev, F. Yildiz, S. Kazan, B. Aktas, A. Gupta, L. R. Tagirov, D. Rata, D. Buegler, P. Gruenberg, C. M. Schneider, S. Kämerer, G. Reiss, and A. Hüten, *Phys. Status Solidi A* **203**, 1503 (2006).